

Compositional and structural systematics of the columbite group

T. SCOTT ERCIT

Research Division, Canadian Museum of Nature, Ottawa, Ontario K1P 6P4, Canada

MICHAEL A. WISE

Department of Mineral Sciences, Smithsonian Institution, Washington, DC 20560, U.S.A.

PETR ČERNÝ

Department of Geological Sciences, University of Manitoba, Winnipeg, Manitoba R3T 2N2, Canada

ABSTRACT

The systematics of the columbite group have been studied to quantify variations in composition and structure. Multiple regression methods involving 89 heated samples and five synthetic equivalents of columbite-group minerals give equations that permit prediction of the effects of composition on unit-cell parameters for fully ordered samples. The results are: $a_0 = 14.258 + 0.166\text{Mn}/(\text{Mn} + \text{Fe}) + 0.0072\text{Ta}/(\text{Ta} + \text{Nb}) - 0.06\text{Ti} - 0.02\text{Sn} + 0.05\text{Sc}$; $b_0 = 5.7296 + 0.031\text{Mn}/(\text{Mn} + \text{Fe}) + 0.0024\text{Ta}/(\text{Ta} + \text{Nb}) - 0.024\text{Ti} - 0.009\text{Sn} + 0.02\text{Sc}$; $c_0 = 5.0495 + 0.033\text{Mn}/(\text{Mn} + \text{Fe}) + 0.011\text{Ta}/(\text{Ta} + \text{Nb}) - 0.004\text{Ti}$, where a_0 , b_0 , and c_0 are the cell parameters (Å) calculated from unit-cell concentrations of elements. With these equations, crystal-chemical trends, the effects of heating experiments, the degree of cation order, and the structural effects of heterovalent cation substitution can be predicted for samples of columbite-group minerals.

INTRODUCTION

The columbite group of minerals has the general formula AB_2O_6 , in which, most typically, A represents Fe^{2+} , Mn, and Mg, and B represents Nb and Ta. Members of the columbite group are subdivided on the basis of A- and B-site chemistry; samples with Nb as the dominant B cation are loosely referred to as "columbite," and with Ta, as "tantallite." In the construction of species names, prefixes are used to describe A-site chemistry; thus, the species of "tantallite" with Mn dominant at the A site is manganotantallite. Columbite-group minerals show variable degrees of cation order. A range of structural states is possible, yet formal guidelines for structural subdivision of the group have not yet been devised. For the purposes of the present paper, samples with intermediate degrees of cation order are referred to as "partially ordered" in conjunction with the name of an ordered species. Thus, "fully disordered ferrocolumbite," "partially ordered ferrocolumbite," and "ferrocolumbite" would describe increasingly cation-ordered variants of the composition FeNb_2O_6 .

The degree of cation order in samples of columbite-group minerals can be judged qualitatively from the relative intensity of supercell reflections, from the ratio of the a cell edge to the c cell edge (Komkov, 1970), or from plots of c vs. a (Černý and Turnock, 1971). The a - c plot can be used to evaluate both cation order and the ratio of Mn:Fe (Fig. 1). However, it has not been used to provide quantitative estimates of these parameters because (1) the range of cell parameters for fully disordered sam-

ples is not known exactly, and (2) the effect of substituents Ti, Sn, and Sc upon cell parameters is not known. Heating of samples in excess of 950 °C has been shown to induce cation order (Nickel et al., 1963); under anhydrous conditions at 1 atm, there seems to be a substantial activation energy that impedes ordering, hence high temperatures are required.

Most variation in the composition of columbite-group minerals is owing to the substitution of Mn for Fe and of Ta for Nb. This is traditionally represented graphically in the form of the columbite quadrilateral (Fig. 2). A compositionally dependent phase transformation exists within the space represented by the quadrilateral. Ignoring cation disorder, the structures involved are those of columbite, which is stable as a single phase over approximately 75% of compositional space, and tapiolite, which is stable as a single phase over 5% of compositional space. A large two-phase region separates the generally (Fe,Ta)-rich tapiolite from members of the columbite-group (Černý et al., 1992).

Previous studies of the systematics of the columbite group have focused on isolated aspects of the topic. Some studies have dealt with the effects of composition upon the unit-cell parameters of fully ordered columbite-group minerals and their synthetic equivalents (e.g., Brandt, 1943; Turnock, 1966; Wise et al., 1985). Some structural studies have been made of columbite-group minerals and their synthetic equivalents, involving ordered (Sturdivant, 1930; Grice et al., 1976; Weitzel, 1976), partially ordered (Wenger et al., 1991), and disordered compositions (Grice et al., 1976). Ercit (1986) quantified com-

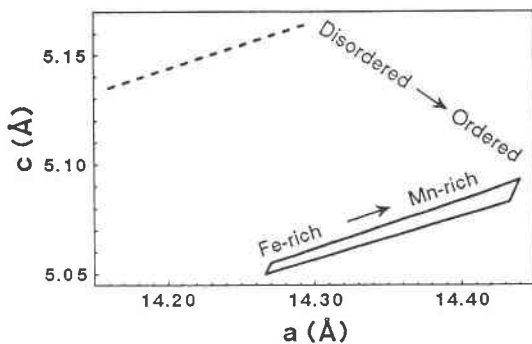


Fig. 1. The a - c diagram for columbite-group minerals. The line at the top of the diagram represents the anticipated upper bound for (fully) disordered samples devoid of impurity elements such as Sn and Ti; the box at the bottom represents the range for ordered impurity-free samples (Wise et al., 1985). Fe-rich samples plot at low values of a , Mn-rich samples at higher values of a .

positional-structural relationships for columbite-group minerals of all ordering states; results of the study were of high precision, but of limited application or accuracy because the effects of common impurity elements (e.g., Sn, Ti, Sc) were not taken into account. We present here a study of the systematics of the columbite group that addresses both normal compositional variations and the variable effects of cation order.

EXPERIMENTAL METHODS

Heating experiments

Heating experiments were performed using a Fisher Isotemp Model 186 muffle furnace. Ag-Pd foil was used as a substrate for all samples. The furnace temperature was periodically calibrated by monitoring the melting point of NaCl. Temperature regulation by the furnace was precise to ± 20 °C. The experiments were performed on coarse crystal fragments in air at 1000 °C for 16 h. Heating under these conditions induces cation order in columbite and results in no significant oxidation of bulk Fe^{2+} , as monitored by unit-cell parameters (Černý and Turnock, 1971; Černý et al., 1986).

Chemical analysis

All chemical analyses were conducted with a MAC 5 electron microprobe; most of these were made by energy dispersion (ED). The oldest analyses (approximately 5% of the total data set) were made by wavelength dispersion (WD).

A Kevex Micro-X 7000 spectrometer was used for ED X-ray analyses. Spectra were collected for 200 live s with an operating voltage of 15 kV and a sample current of 5 nA (measured on synthetic fayalite), and they were corrected for both current and voltage drift. Analytical precision at the 2σ level was typically 1% for Ta and Nb in major concentrations and 2% for Mn and Fe in major concentrations and Ta and Nb in minor concentrations. Analytical precision was typically poorer than 2% for Ti,

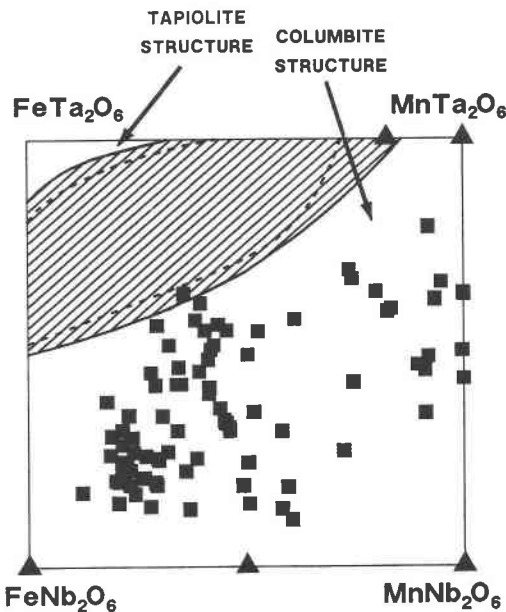


Fig. 2. The columbite quadrilateral. A large two-phase region (shaded) separates compositions with the tapiolite structure from those with the columbite structure: solid lines for coexisting tantalite and tapiolite, dashed lines for single phases (after Černý et al., 1992). The compositions of samples used in the present study are shown as squares for natural samples and triangles for synthetic samples.

Sn, Sc, and Ca. Line overlaps, such as $\text{Ta}M\delta$ and $\text{Ta}M_N$ on $\text{Nb}L\alpha$, $\text{Sn}L\beta$ on $\text{Ti}K\alpha$, and $\text{Mn}K\beta$ on $\text{Fe}K\alpha$ were separated by noniterative techniques of spectral stripping involving the library spectra of individual elements taken from standards used in the analysis of columbite-group minerals. The data were reduced with Kevex software using the MAGIC V program (Colby, 1980). The standards were manganotantalite ($\text{Mn}K\alpha$, $\text{Ta}M\alpha$), CoNb_2O_6 ($\text{Nb}L\alpha$), synthetic fayalite ($\text{Fe}K\alpha$), rutile ($\text{Ti}K\alpha$), cassiterite ($\text{Nb}L\alpha$), scandium metal ($\text{Sc}K\alpha$), and microlite ($\text{Ca}K\alpha$). No other element with $Z > 10$ was detected in the 200 s spectrum.

WD X-ray analyses were performed under the following conditions: 20 kV, 40 nA (measured on brass), and 10-s count time. The data were reduced with a modified version of the EMPADR VII program (Rucklidge and Gasparrini, 1969). The standards were manganotantalite ($\text{Mn}K\alpha$, $\text{Ta}L\alpha$), CaNb_2O_6 ($\text{Ca}K\alpha$, $\text{Nb}L\alpha$), chromite ($\text{Fe}K\alpha$), titanite ($\text{Ti}K\alpha$), and scandium metal ($\text{Sc}K\alpha$). Whenever possible, multiple chemical analyses were made on each sample and averaged to give a bulk composition.

Powder X-ray diffraction analysis

Powder X-ray diffraction (XRD) experiments were performed using Philips PW1050 and PW1710 powder diffractometers. Experiments involving the PW1050 used fixed divergence slits, Ni-filtered $\text{Cu}K\alpha$ radiation, and a scan speed of $1/4^\circ 2\theta/\text{min}$; manually measured 2θ readings

were taken from diffractograms. Experiments involving the PW1710 used a variable divergence slit (coupled to the θ - 2θ drive), monochromated $\text{CuK}\alpha$ radiation, and a scan speed of $0.01^\circ 2\theta/\text{s}$; 2θ readings were automatically measured by computer. Precision of measurement was estimated to be ± 0.02 to $\pm 0.04^\circ 2\theta$ for experiments involving the PW1050, and ± 0.01 to $\pm 0.03^\circ 2\theta$ for experiments involving the PW1710. For all experiments, annealed CaF_2 was used as an internal standard [$a = 5.46379(4) \text{ \AA}$]. Indexing and refinement of unit-cell parameters were done with the CELREF program (Appleman and Evans, 1973). Sharp peaks of normal width at half height were assigned unit weights; ragged or abnormally broad peaks were assigned variable weights, which depended upon the quality of the peak. Peaks that were obviously in an overlapping relationship were omitted from the refinement. Least-squares refinement typically involved data from 10 to 18 reflections, with the lower end of the range representing disordered samples, and the upper end, ordered samples.

STATISTICAL ANALYSIS

Sample selection

For the study of the effect of composition upon the unit-cell parameters of fully ordered and heated samples of columbite-group minerals, compositional and powder XRD data were collected on 100 samples taken from 31 groups of granitic pegmatites (Černý et al., 1986; Ercit, 1986; Wise, 1987). This data set was augmented with powder XRD data for five synthetic samples (Wise et al., 1985). The total data set was examined carefully for consistency and sample quality: (1) The compositional data for all samples were examined. One sample did not fit columbite stoichiometry well in that it had significantly deficient A-site sums, which suggests cation leaching. One sample had an abnormally high Ca content, implying alteration to pyrochlore. Both samples were omitted from the data set. (2) The standard deviations in the refined unit-cell parameters of all samples were examined. Five samples with unacceptably large standard deviations, indicative of poor crystallinity, compositional inhomogeneity, or admixture with other phases, were omitted from the data set. (3) The XRD data for unheated and heated pairs were plotted in an a - c graph (Fig. 3a). Four samples had heating vectors with slopes that deviated strongly from the norm, yet for which no obvious explanation could be found. It was assumed that these samples were compositionally inhomogeneous, i.e., that the unheated fragment did not have exactly the same composition as the fragment used in the heating experiments, hence yielding the deviant slopes. These samples were omitted from the data set. The final data set consisted of 89 unheated and five synthetic samples. Figure 3b is an a - c plot for unheated samples only and shows that the data set covers a broad range of states of cation order. Figure 2 shows that the data set covers a similarly broad range of compositional space.

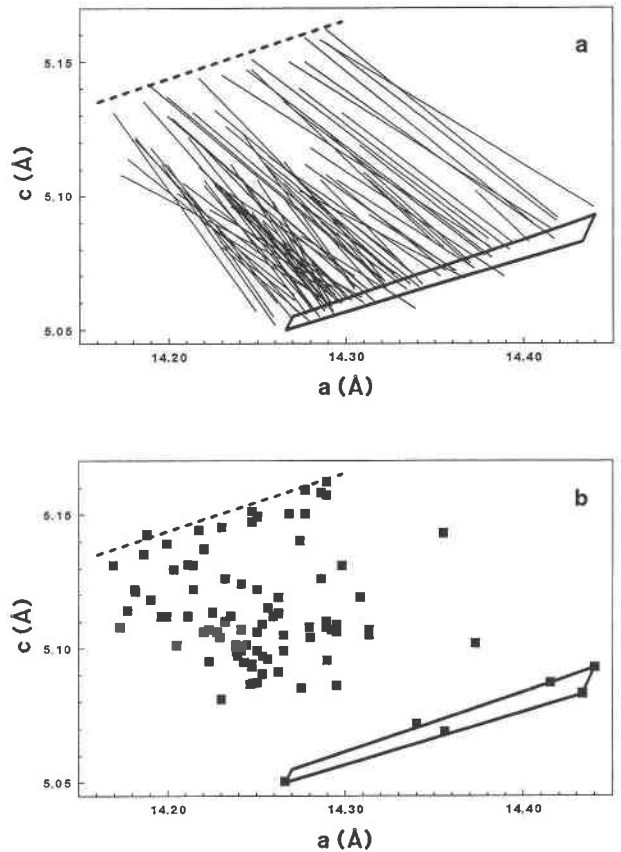


Fig. 3. Powder XRD data for samples of columbite-group minerals used in the present study. (a) Heating paths for unheated and heated pairs; unheated samples plot at the upper left end of each path, heated samples at the lower right end. (b) Data for unheated samples only, showing the range of structural states shown by the data set.

Multiple regression analysis

Multiple regression analysis was performed using SYSTAT for DOS systems (version 5.0). To minimize parameter correlation, the independent variables were chosen on the basis of deviation from an FeNb_2O_6 end-member. We selected as variables the ratios $\text{Mn}/(\text{Mn} + \text{Fe})$ and $\text{Ta}/(\text{Ta} + \text{Nb})$ and the unit-cell concentrations of Sc, Sn, and Ti. $\text{Mn}/(\text{Mn} + \text{Fe})$ and $\text{Ta}/(\text{Ta} + \text{Nb})$ were used instead of the unit-cell concentrations of Mn and Ta in anticipation of the application of the results of the study to compositions of columbite-group minerals that fall outside the limits of our data set (e.g., Zr- and W-bearing samples).

The order of each equation was determined by backward elimination. A standard value of α was used (0.15) in deciding whether or not a variable contributed significantly to the model. For the data set as a whole, it was found that the $\text{Nb} = \text{Ta}$ substitution results in no significant change in the a and b cell parameters. However, the study of Wise et al. (1985) showed that for synthetic co-

TABLE 1. Results of multiple regression analysis

Dependent variable	Intercept	Independent variables and coefficients					R^2 (%)
		MnFe	TaNb	Ti	Sn	Sc	
a_{Nb}	14.258	0.166	0	-0.06	-0.02	0.05	93
b_{Nb}	5.7296	0.031	0	-0.024	-0.009	0.02	86
c	5.0495	0.033	0.011	-0.004	0	0	90
Statistical data							
a_{Nb}	3(0.0)	5(0.0)	—	1(0.0)	1(10.7)	3(13.3)	
b_{Nb}	9(0.0)	1(0.0)	—	3(0.0)	4(2.8)	1(5.0)	
c	9(0.0)	2(0.0)	2(0.0)	2(5.4)	—	—	

Note: for the statistical data, leading numbers are standard deviations on the last significant figure of the corresponding parameters above. Numbers in parentheses are percent probabilities for $H_0|t| = 0$. MnFe = Mn/(Mn + Fe); TaNb = Ta/(Ta + Nb).

lumbite-tantalite, substitution of Ta for Nb results in a slight expansion of both a and b . Consequently, the values of a and b used in the regression analysis were modified to reflect the effect of the Nb = Ta substitution shown by synthetic columbite-tantalite,

$$a_{Nb} = a_H - 0.007(5)Ta/(Ta + Nb) \quad (1)$$

$$b_{Nb} = b_H - 0.0024(4)Ta/(Ta + Nb) \quad (2)$$

where a_H and b_H are the measured a and b cell edges for heated samples, and a_{Nb} and b_{Nb} are the modified variables used in the regression analysis (all in ångströms); the coefficients of the equations were derived by regression of data in Wise et al. (1985). For the final stage it was found that all variables contribute significantly to a and b , but that only Mn/(Mn + Fe), Ta/(Ta + Nb), and Ti content per unit cell contribute significantly to c . The coefficients, the intercepts for the multiple regression models, and statistical information are given in Table 1; the data set used in the regression analysis is given in Table 2.¹ In addition to the data in Table 1, the relative success of the analysis is shown by the high proportion of significant variables, by the high values of the correlation coefficients and by the low standard errors of the estimates. The root mean square errors in a , b , and c are 0.012, 0.004, and 0.003 Å, respectively.

The following equations result when the data in Table 1 are combined with Equations 1 and 2:

$$\begin{aligned} a_0 = & 14.258 + 0.166Mn/(Mn + Fe) \\ & + 0.0072Ta/(Ta + Nb) - 0.06Ti \\ & - 0.02Sn + 0.05Sc \end{aligned} \quad (3)$$

$$\begin{aligned} b_0 = & 5.7296 + 0.031Mn/(Mn + Fe) \\ & + 0.0024Ta/(Ta + Nb) - 0.024Ti \\ & - 0.009Sn + 0.02Sc \end{aligned} \quad (4)$$

$$\begin{aligned} c_0 = & 5.0495 + 0.033Mn/(Mn + Fe) \\ & + 0.011Ta/(Ta + Nb) - 0.004Ti \end{aligned} \quad (5)$$

where Ti, Sc, and Sn represent the number of atoms per unit cell for these elements, and a_0 , b_0 , and c_0 represent the calculated values (in ångströms) of a , b , and c for heated or fully ordered members of the columbite group. Figure 4 shows the correspondence between observed and calculated values of a , b , and c . The plots are generally linear; however, there is an appearance of decreased slopes at the extreme ends of each plot, which might indicate slight positive and negative excess volumes of mixing for Mn = Fe substitution. Alternately, the apparent deviations may simply be a sampling artifact (the deviations are defined by only two or three points).

APPLICATIONS

Crystal chemistry of ordered columbite-group minerals

Relative to an FeNb₂O₆ end-member, Equations 3–5 show consistent behavior for all substituents. Substitution of Mn for Fe and of Ta for Nb generally causes cell parameters to increase. On the basis of the ionic radii of Shannon (1976) this behavior is predicted for Mn = Fe substitution, but no change is predicted for substitution of Ta for Nb. The present study indicates that the sixfold-coordinated ionic radius for Ta is actually slightly larger than that of Nb. Entry of Ti or Sn in the columbite structure causes all cell parameters to decrease. This again can be predicted from the ionic radii of Shannon (1976). For the samples studied here, Ti and Sn are expected to substitute at both the A and B sites as a MO₂ component (M = Ti, Sn); the ionic radii of Ti (0.605 Å) and Sn (0.69 Å) are less than or equal to the weighted mean cation radius for ferrocolumbite (0.69 Å).

Entry of Sc in the columbite structure causes a and b to increase (no significant effect upon c). The behavior of Sc in the columbite structure is not well understood. Sc has a sixfold-coordinated ionic radius of 0.745 Å (Shannon, 1976); if Sc substitutes only at the A site, then we would predict a decrease in cell volume, exactly the opposite of what is observed with substitution of Sc for Fe²⁺ ($r = 0.78$ Å; Shannon, 1976). The volume increase in our model concomitant with Sc substitution indicates that Sc enters both the A and B cation sites in cation-ordered columbite-group minerals.

Equations 3–5 illustrate some of the problems with graphical methods for making inferences about A-site

¹ A copy of Table 2 may be ordered as Document AM-95-587 from the Business Office, Mineralogical Society of America, 1130 Seventeenth Street NW, Suite 330, Washington, DC 20036, U.S.A. Please remit \$5.00 in advance for the microfiche.

chemistry. Calculations show that a columbite sample with a Mn:Fe ratio of 0.20 and containing only 0.40 Ti atoms per unit cell falls in the same area of an a - c plot as end-member ferrocolumbite. Thus, by ignoring the minor element chemistry of columbite-group minerals in the use of plots like Figure 1, major errors can result in estimating geochemically important information, such as Mn:Fe ratios.

Prediction of the effects of heating experiments

Although it is generally possible to perform heating experiments on samples of columbite-group minerals, there are many cases in which such experiments cannot be done, such as (1) too little sample for powder XRD work on both unheated and heated chips, (2) samples with strong compositional zoning, and (3) samples with intergrowths or inclusions of other phases. By using the equations presented in the previous section, unit-cell parameters can be predicted for heated samples with only compositional data as the input.

As both a - c plots and the calculations show, increased cation order caused by heating results in increased values of a and decreased values of c . This can be explained by consideration of patterns in cation order relative to the hexagonal closest-packing of anions in the columbite structure. For all ordering variants of the columbite structure (Grice et al., 1976), coordination polyhedra (octahedra) share edges to form zig-zag chains parallel to c . These chains are linked to adjacent chains by corner sharing along a and b . Disordered variants (ixiolite structure) have a random distribution of cations within these chains, whereas ordered variants (columbite structure) have only one type of cation within all chains of a given (100) layer of the structure. Thus, heating of an incompletely ordered sample results in a more efficient packing of cations along the chains, hence a reduction in c . However, cation ordering also results in compositional differences between adjacent A-cation-bearing and B-cation-bearing (100) layers. Thus, layer misfit is greater for cation-ordered variants than for their disordered equivalents; hence an increase in a is observed with increased cation order.

Estimation of the degree of cation order

The degree of cation order (Q) in columbite-group minerals is traditionally assessed by the relative position on an a - c plot. By comparing the location of a point to the lines for fully ordered and fully disordered samples of columbite-group minerals, it is possible to state whether one sample is more ordered than another and whether a sample is largely cation-ordered or largely disordered. Quantification of the degree of cation order is complicated by a number of factors: (1) Unit-cell parameters for disordered samples are not precisely known. To date, only fully ordered samples of columbite-group minerals have been successfully synthesized. Furthermore, only one study exists in which the degree of cation order in columbite-group minerals was refined (Wenger et al., 1991). Consequently, the only estimates of the unit-cell param-

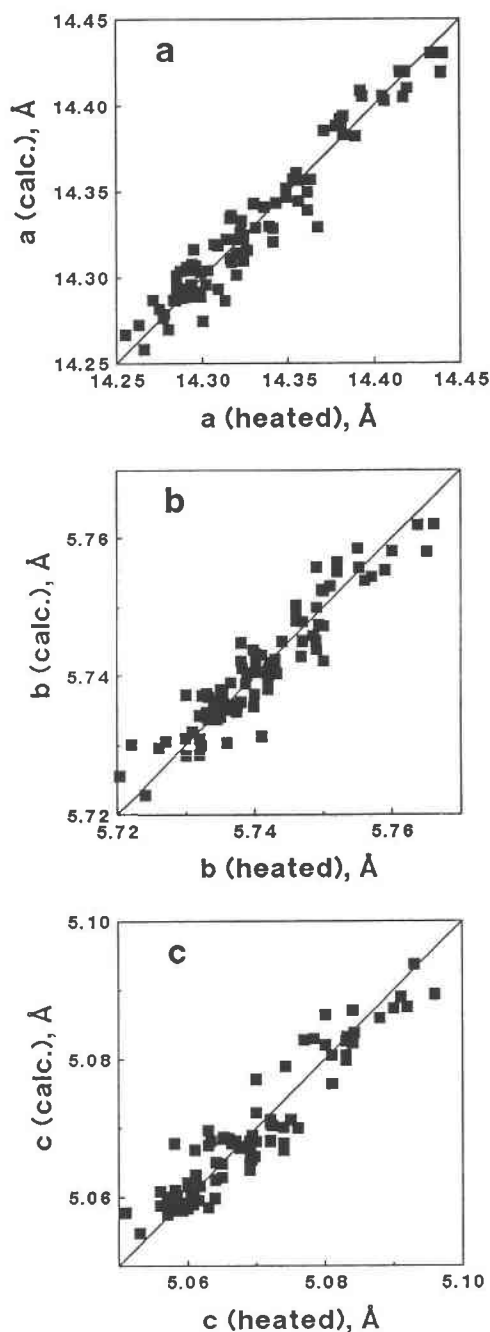


Fig. 4. Plots of calculated vs. observed unit-cell parameters (a , b , and c) for samples used in the regression analysis.

eters for fully disordered members of the columbite group have been made by trial-and-error, i.e., by XRD experiments on samples that plot farthest from the ordered field in the a - c plot and show no supercell reflections (e.g., Černý and Ercit, 1989). (2) The effects of impurity elements such as Ti, Sn, and Sc upon unit-cell parameters of columbite-group minerals are largely unknown. Using then-current estimates of the unit-cell parameters for disordered $\text{Mn}(\text{Ta},\text{Nb})_2\text{O}_6$ and $\text{Fe}(\text{Nb},\text{Ta})_2\text{O}_6$, Ercit (1986)

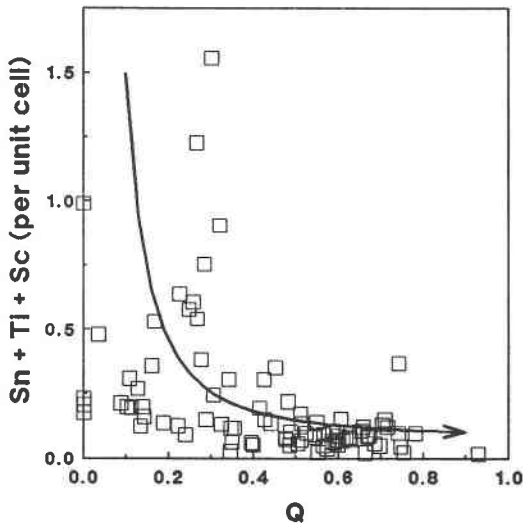


Fig. 5. Plot of total number of impurity elements vs. degree of cation order. Although compositions poor in impurity elements show a broad range of structural states, compositions rich in impurity elements show low to medium degrees of cation order.

quantified the a - c graph for compositions devoid of impurity elements. However, because the quantification was largely graphical rather than algebraic in approach, and because the effects of the most common impurity elements upon the columbite structure are now known, we attempt to requantify order-disorder relationships for columbite-group minerals.

The approach taken by Ercit (1986) was essentially one of assigning a figure for the degree of cation order by measuring the relative distance of a data point in an a - c graph from the lines characterizing the ordered and disordered fields. This was quantified as

$$\text{percent order} = 1727 - 941.6(c - 0.2329a). \quad (6)$$

An alternate approach to the problem, and one which is better suited to samples with moderate concentrations of impurity elements, involves determining the magnitude of the heating vector. In structural space, the magnitude of the heating vector ($|\mathbf{h}|$, in ångströms) is simply

$$|\mathbf{h}| = [(a_U - a_H)^2 + (b_U - b_H)^2 + (c_U - c_H)^2]^{1/2} \quad (7)$$

where the subscripts U and H refer to unheated and heated samples, respectively. For heated samples, the equation can contain either experimentally determined values of a , b , or c or the values estimated from Equations 3–5, above.

If we assume, for the purposes of the present study, that dV/dQ is independent of chemistry, then the degree of cation order for a given sample can be calculated by comparing the magnitude of its heating vector to that of a fully disordered sample. Presently, the magnitude of a heating vector for a fully disordered sample is not known; however, it can be approximated as the maximum ob-

served heating vector for the data set. There are two candidates for this maximum: samples TRT-42 and SF21. Although the vector magnitude for sample TRT-42 is slightly greater than for sample SF21, the latter sample was chosen to represent the fully disordered standard because powder XRD experiments showed TRT-42 to be slightly contaminated, and the choice of sample SF21 as the standard results in a better fit to the ordering data from the crystal structure refinements of Wenger et al. (1991). The magnitude of the heating vector for sample SF21 is 0.166 Å. The degree of order of any sample of a columbite-group mineral can then be estimated by

$$Q = 1 - (|\mathbf{h}|/0.166). \quad (8)$$

Values of Q range from 0 (completely disordered) to 1 (completely ordered). If Equations 3–5 are used to calculate the unit-cell parameters for heated samples, and if the powder XRD experiments for unheated samples are conducted as described in the Experimental Methods section (powder diffractometry, CaF_2 standard), then the standard error of estimation of Q is 0.08 (cf. 0.03 if measured values of a_H , b_H , and c_H are used). The quality of the result can be judged by comparison of calculated Q values with observed values from the structure refinements of Wenger et al. (1991). With unit-cell parameters for the single crystals used in the refinements, and using the correct composition for sample NCPI, we obtain the following. For sample NCPI, $Q_{\text{obs}} = 0.46$ vs. $Q_{\text{calc}} = 0.51$, and for sample NCP5, $Q_{\text{obs}} = 0.31$ vs. $Q_{\text{calc}} = 0.25$. There is good agreement considering that single-crystal diffractometer data were used rather than powder diffractometer data and that sample NCPI of Wenger et al. (1991) is compositionally inhomogeneous.

Impurity elements and cation order

To date, the causes of cation disorder in columbite-group minerals are poorly understood, as is the role of impurity elements in the disorder process. Figure 5 is a plot of the sum of impurity elements in the columbite structure vs. the degree of cation order. The plot shows considerable compositional scatter at the low- Q end of the diagram and much less scatter at the high- Q end. Although compositions with low concentrations of these elements show a full range of structural states, compositions with high concentrations of impurity elements show only low to moderate degrees of order. Ultimately, the question is one of whether the correlation is largely crystal-chemical or geochemical in origin; i.e., do the heterovalent substitution mechanisms necessary for the introduction of impurity elements to columbite structure induce cation disorder, or do columbite-group minerals with high levels of impurity elements form relatively early in the crystallization histories of granites and pegmatites, at a time when disordered states are more stable for columbite-group minerals? The answer may come from studying a broader range of rock types (e.g., columbite-group minerals from granites, carbonatite suites, and kimberlites).

ACKNOWLEDGMENTS

Specimens used in this study were collected during projects financed by the Canada-Manitoba DREE program 1975–1980, by research agreements from the Geology Office, INAC Yellowknife 1981–1986, by NSERC operating grants to P.Č., and by NSERC postgraduate scholarships to T.S.E. Laboratory studies were funded by Canadian Museum of Nature RAC grants to T.S.E. and NSERC operating grants and DEMR research agreements to P.Č. We thank E.E. Foord and an anonymous referee for comments, which improved the quality of the manuscript.

REFERENCES CITED

- Appleman, D.E., and Evans, H.T., Jr. (1973) Job 9214: Indexing and least-squares refinement of powder diffraction data. U.S. National Technical Information Service, Document PB 216-188.
- Brandt, K. (1943) X-ray studies on ABO_4 compounds of rutile type and AB_2O_6 compounds of columbite type. *Arkiv för Kemi Mineralogi och Geologi*, 17A(15), 1–8.
- Černý, P., and Ercit, T.S. (1989) Mineralogy of niobium and tantalum: Crystal chemical relationships, paragenetic aspects and their economic implications. In P. Möller, P. Černý, and F. Saupé, Eds., *Lanthanides, tantalum and niobium*, p. 27–79. Springer-Verlag, Berlin.
- Černý, P., and Turnock, A.C. (1971) Niobium-tantalum minerals from granitic pegmatites at Greer Lake, southeastern Manitoba. *Canadian Mineralogist*, 10, 755–772.
- Černý, P., Goad, B.E., Hawthorne, F.C., and Chapman, R. (1986) Fractionation trends of the Nb- and Ta-bearing oxide minerals in the Greer Lake pegmatitic granite and its pegmatite aureole, southeastern Manitoba. *American Mineralogist*, 71, 501–517.
- Černý, P., Ercit, T.S., and Wise, M.A. (1992) The tantalite-tapiolite gap: Natural assemblages versus experimental data. *Canadian Mineralogist*, 30, 587–596.
- Colby, J.W. (1980) MAGIC V: A computer program for quantitative electron-excited energy dispersive analysis. In *QUANTEX-Ray Instruction Manual*. Kevex Corporation, Foster City, California.
- Ercit, T.S. (1986) The simpsonite paragenesis: The crystal chemistry and geochemistry of extreme Ta fractionation. Ph.D. thesis, University of Manitoba, Winnipeg, Canada.
- Grice, J.D., Ferguson, R.B., and Hawthorne, F.C. (1976) The crystal structures of tantalite, ixiolite and wodginite from Bernic Lake, Manitoba: I. Tantalite and ixiolite. *Canadian Mineralogist*, 14, 540–549.
- Komkov, A.I. (1970) Relationship between the X-ray constants of columbites and composition. *Doklady Akademii Nauk SSSR*, 195, 117–119.
- Nickel, E.H., Rowland, J.F., and McAdam, R.C. (1963) Ixiolite—A columbite substructure. *American Mineralogist*, 48, 961–979.
- Rucklidge, J., and Gasparrini, E. (1969) Specifications of a computer program for processing electron micro-probe analytical data (EMPADR VII). Department of Geology, University of Toronto, Toronto, Canada.
- Shannon, R.D. (1976) Revised effective ionic radii and systematic studies of interatomic distances in halides and chalcogenides. *Acta Crystallographica*, A32, 751–767.
- Sturdivant, J.H. (1930) The crystal structure of columbite. *Zeitschrift für Kristallographie*, 75, 88–105 (in German).
- Turnock, A.C. (1966) Synthetic wodginite, tapiolite and tantalite. *Canadian Mineralogist*, 8, 461–470.
- Weitzel, H. (1976) Kristallstrukturverfeinerung von Wolframiten und Columbiten. *Zeitschrift für Kristallographie*, 144, 238–258.
- Wenger, M., Armbruster, T., and Geiger, C.A. (1991) Cation distribution in partially ordered columbite from the Kings Mountain pegmatite, North Carolina. *American Mineralogist*, 76, 1897–1904.
- Wise, M.A. (1987) Geochemistry and crystal chemistry of Nb, Ta and Sn minerals from the Yellowknife pegmatite field, N.W.T. Ph.D. thesis, University of Manitoba, Winnipeg, Canada.
- Wise, M.A., Turnock, A.C., and Černý, P. (1985) Improved unit cell dimensions for ordered columbite-tantalite end members. *Neues Jahrbuch für Mineralogie Monatshefte*, 372–378.

MANUSCRIPT RECEIVED MAY 13, 1994

MANUSCRIPT ACCEPTED JANUARY 23, 1995

AM-95-587

Compositional and structural systematics of the columbite group

T. Scott Ercit, Michael A. Wise, Petr Cerny

For deposit: Table 2

American Mineralogist, 80, 5-6, 613-619.

TABLE 2. Data used in multiple regression analysis (FOR DEPOSITION)

SAMPLE	UNHEATED			HEATED			CALCULATED			CATIONS PER UNIT CELL								
	a	b	c	a(H)	b(H)	c(H)	a(H)	b(H)	c(H)	Ta	Nb	Ti	Sn	Sc	Fe3+	Fe2+	Mn	Ca
ANN-N-1	14.290	5.736	5.095	14.326	5.743	5.069	14.316	5.740	5.064	2.54	5.44	0.02	0.00	0.00	0.00	2.65	1.37	0.00
BET-4				14.324	5.733	5.063	14.312	5.738	5.068	5.03	2.86	0.11	0.12	0.00	0.00	2.46	1.36	0.00
BET-15	14.223	5.729	5.095	14.309	5.737	5.064	14.296	5.735	5.061	2.00	5.72	0.11	0.07	0.00	0.51	2.64	0.97	0.00
BET-104	14.247	5.733	5.093	14.291	5.735	5.058	14.290	5.735	5.059	1.93	6.01	0.08	0.00	0.00	0.00	3.15	0.85	0.00
BET-105	14.239	5.731	5.097	14.289	5.734	5.057	14.291	5.735	5.059	1.87	6.08	0.07	0.00	0.00	0.00	3.14	0.85	0.00
BET-107	14.241	5.729	5.099	14.293	5.738	5.061	14.296	5.736	5.060	2.40	5.56	0.04	0.02	0.00	0.00	3.02	0.94	0.00
BET-111	14.243	5.728	5.095	14.294	5.737	5.061	14.295	5.736	5.060	2.11	5.81	0.07	0.01	0.00	0.00	3.07	0.97	0.00
BIG-A-1	14.256	5.738	5.115	14.353	5.746	5.070	14.355	5.748	5.072	2.51	5.47	0.02	0.01	0.00	0.00	1.68	2.34	0.00
BIG-B-15	14.214	5.730	5.122	14.303	5.732	5.061	14.305	5.737	5.063	2.80	5.13	0.10	0.01	0.00	0.00	2.74	1.21	0.00
BILL-2-9	14.199	5.723	5.112	14.263	5.730	5.057	14.271	5.728	5.057	1.15	6.57	0.35	0.00	0.00	0.00	3.18	0.83	0.00
BILL-2-13	14.196	5.722	5.112	14.300	5.726	5.051	14.274	5.729	5.057	1.56	6.20	0.29	0.02	0.00	0.00	3.20	0.80	0.00
BILL-5-9A	14.190	5.725	5.118	14.275	5.730	5.057	14.281	5.731	5.058	1.33	6.48	0.28	0.03	0.00	0.00	2.94	0.95	0.00
BILL-5-12	14.220	5.728	5.106	14.285	5.732	5.057	14.292	5.734	5.059	1.10	6.70	0.20	0.02	0.00	0.00	2.93	1.13	0.00
CAS-A-4	14.256	5.733	5.096	14.299	5.735	5.061	14.303	5.737	5.063	3.59	4.32	0.07	0.04	0.00	0.00	2.90	1.13	0.00
CAS-A-10	14.250	5.731	5.099	14.291	5.735	5.060	14.306	5.738	5.062	2.02	5.94	0.05	0.02	0.00	0.00	2.77	1.17	0.00
CATA-K-1	14.286	5.743	5.126	14.371	5.751	5.074	14.383	5.753	5.079	3.42	4.53	0.02	0.04	0.00	0.00	1.02	2.99	0.00
FLY-1-11	14.241	5.731	5.124	14.314	5.738	5.065	14.324	5.742	5.069	4.91	3.06	0.05	0.01	0.00	0.00	2.40	1.56	0.00
FREDA-3	14.253	5.732	5.109	14.320	5.742	5.069	14.314	5.740	5.065	3.40	4.55	0.03	0.06	0.00	0.00	2.62	1.35	0.00
FREDA-14	14.340	5.747	5.072	14.341	5.747	5.072	14.329	5.743	5.068	3.88	4.12	0.00	0.02	0.00	0.00	2.34	1.64	0.00
G69-30	14.277	5.750	5.159	14.405	5.757	5.090	14.402	5.754	5.086	4.86	2.93	0.22	0.04	0.00	0.00	0.27	3.74	0.00
G69-55	14.289	5.753	5.157	14.418	5.760	5.091	14.420	5.758	5.089	5.01	2.87	0.11	0.08	0.00	0.00	0.00	3.91	0.00
G69-61	14.286	5.755	5.158	14.439	5.765	5.096	14.418	5.758	5.089	5.02	2.84	0.14	0.06	0.00	0.00	0.01	3.94	0.00
GL2A-17	14.247	5.739	5.147	14.349	5.742	5.083	14.352	5.741	5.079	5.07	2.50	0.51	0.06	0.00	0.00	1.01	2.92	0.00
GL2A-18	14.247	5.739	5.147	14.349	5.742	5.083	14.350	5.740	5.079	5.25	2.34	0.52	0.08	0.00	0.00	1.01	2.81	0.00
GL8C31-6	14.173	5.709	5.108	14.299	5.732	5.064	14.284	5.727	5.062	1.86	5.47	0.89	0.00	0.34	0.00	2.09	1.31	0.00
GL9-19	14.177	5.716	5.114	14.271	5.724	5.063	14.284	5.722	5.069	3.85	3.16	1.08	0.28	0.19	0.00	1.65	1.83	0.00
GL9-20	14.186	5.723	5.135	14.285	5.722	5.061	14.294	5.730	5.066	3.16	4.38	0.52	0.12	0.00	0.00	2.27	1.61	0.00
GL12-1	14.217	5.722	5.144	14.320	5.732	5.074	14.298	5.730	5.066	2.40	5.01	0.69	0.08	0.13	0.00	2.02	1.73	0.00
GL12A-1	14.247	5.741	5.151	14.380	5.746	5.084	14.394	5.751	5.087	6.09	1.60	0.28	0.20	0.00	0.00	0.31	3.52	0.00
GR2MNA	14.275	5.728	5.085	14.339	5.738	5.058	14.329	5.742	5.068	2.94	4.99	0.06	0.04	0.00	0.00	2.24	1.75	0.00
GR30A1	14.230	5.725	5.081	14.280	5.736	5.053	14.270	5.730	5.055	1.38	6.55	0.15	0.00	0.00	0.00	3.40	0.48	0.00
JAKE-B-2	14.292	5.744	5.107	14.361	5.749	5.072	14.346	5.744	5.070	1.05	6.82	0.15	0.00	0.00	0.00	1.69	2.34	0.00
JAKE-C-5	14.280	5.741	5.104	14.367	5.750	5.069	14.331	5.742	5.068	2.65	5.28	0.08	0.00	0.00	0.00	2.13	1.77	0.11
JAKE-G-3	14.214	5.730	5.131	14.316	5.743	5.074	14.332	5.742	5.067	1.49	6.40	0.14	0.00	0.00	0.00	2.03	1.97	0.00
JAKE-G-5	14.355	5.768	5.143	14.389	5.750	5.070	14.377	5.751	5.076	2.13	5.79	0.05	0.00	0.00	0.00	1.13	2.96	0.00
JO-A-18	14.253	5.733	5.097	14.302	5.738	5.061	14.296	5.735	5.060	1.65	6.28	0.12	0.00	0.00	0.00	2.90	1.05	0.00
LIT-2-2	14.265	5.738	5.105	14.324	5.742	5.068	14.325	5.742	5.067	3.65	4.33	0.01	0.02	0.00	0.00	2.43	1.56	0.00
LU-A-5	14.295	5.737	5.086	14.323	5.740	5.066	14.333	5.743	5.068	2.73	5.24	0.04	0.01	0.00	0.00	2.19	1.78	0.00
LU-C-19	14.262	5.735	5.091	14.293	5.735	5.056	14.305	5.738	5.061	1.57	6.40	0.04	0.02	0.00	0.00	2.81	1.15	0.00
MAC-109				14.320	5.739	5.069	14.323	5.740	5.069	4.09	3.80	0.13	0.05	0.00	0.00	2.27	1.68	0.00
MAC-111	14.199	5.732	5.139	14.324	5.741	5.072	14.324	5.741	5.068	4.03	3.90	0.10	0.02	0.00	0.00	2.29	1.64	0.00
MAC-112	14.211	5.730	5.131	14.307	5.738	5.070	14.312	5.736	5.070	4.27	3.27	0.11	0.64	0.00	0.00	2.06	1.58	0.00
MAC-115	14.220	5.734	5.137	14.331	5.743	5.074	14.330	5.742	5.070	4.38	3.53	0.11	0.02	0.00	0.00	2.17	1.81	0.00
MEL-1-12	14.247	5.730	5.094	14.294	5.737	5.059	14.290	5.735	5.058	2.09	5.92	0.02	0.00	0.00	0.00	3.18	0.74	0.03
MEL-5-3	14.181	5.721	5.121	14.278	5.731	5.058	14.281	5.732	5.059	3.08	4.88	0.15	0.00	0.00	0.00	3.13	0.69	0.00
MEL-8-5	14.181	5.722	5.122	14.277	5.727	5.063	14.277	5.730	5.058	2.39	5.43	0.24	0.01	0.00	0.00	3.23	0.76	0.00
MEL-9-20	14.235	5.727	5.112	14.287	5.730	5.065	14.305	5.738	5.065	4.48	3.44	0.09	0.02	0.00	0.00	2.83	1.18	0.00
MINT-B-4	14.295	5.740	5.109	14.330	5.738	5.076	14.343	5.745	5.070	2.87	5.11	0.04	0.03	0.00	0.00	1.90	2.03	0.00
MOOSE-7	14.223	5.719	5.107	14.284	5.733	5.058	14.286	5.733	5.058	1.56	6.32	0.12	0.01	0.00	0.00	3.20	0.83	0.00
MOOSE-9	14.228	5.729	5.106	14.285	5.733	5.060	14.291	5.735	5.059	1.90	6.04	0.10	0.00	0.00	0.00	3.07	0.89	0.00
MOOSE-12	14.205	5.728	5.101	14.283	5.735	5.059	14.288	5.734	5.059	2.26	5.68	0.12	0.02	0.00	0.00	3.05	0.83	0.00
MOOSE-16	14.250	5.736	5.087	14.287	5.735	5.059	14.288	5.734	5.059	1.94	5.96	0.12	0.00	0.00	0.00	3.16	0.86	0.00
MOOSE-102A	14.239	5.728	5.101	14.293	5.736	5.061	14.291	5.735	5.059	1.94	5.98	0.07	0.03	0.00	0.00	3.13	0.88	0.00
MOOSE-104A	14.238	5.730	5.101	14.291	5.736	5.060	14.292	5.735	5.059	1.79	6.15	0.09	0.02	0.00	0.00	3.03	0.92	0.00
MOOSE-114A	14.238	5.730	5.099	14.295	5.736	5.060	14.291	5.735	5.059	1.69	6.25	0.06	0.02	0.00	0.00	3.12	0.86	0.00
MOOSE-118	14.248	5.733	5.087	14.289	5.733	5.062	14.289	5.734	5.060	2.53	5.39	0.11	0.02	0.00	0.00	3.11	0.85	0.00
MOOSE-122	14.246	5.734	5.086	14.290	5.736	5.056	14.293	5.735	5.059	1.51	6.43	0.07	0.02	0.00	0.00	3.06	0.92	0.00
MURKY-8	14.253	5.732	5.090	14.296	5.740	5.060	14.292	5.735	5.059	1.65	6.33	0.05	0.00					